A network diagram consisting of various-sized circles connected by thin lines, set against a blue background. The circles are arranged in a non-uniform, interconnected pattern, with some larger circles and some smaller ones. The lines connect the circles, creating a web-like structure.

KWR 2024.044 | February 2024

Fate of PFAS during dune infiltration

Report

Fate of PFAS during dune infiltration

KWR 2024.044 | February 2024

Project number

403936/004

Project manager

Marcelle van der Waals

Client

DPWE-Onderzoeksprogramma 2022

Authors

Elvio Amato, Bas van der Grift

Quality Assurance

Thomas ter Laak

Sent to

DPWE Begeleidingsgroep Waterkwaliteit

This report is distributed to DPWE-participants.
A year after publication it is public.

Keywords

PFAS, dune infiltration, soil, groundwater

[Year of publishing](#)
2024

[More information](#)
Dr. Elvio Amato
T +31 30 606 9754
E elvio.amato@kwrwater.nl

PO Box 1072
3430 BB Nieuwegein
The Netherlands

T +31 (0)30 60 69 511
E info@kwrwater.nl
I www.kwrwater.nl

The logo for KWR, consisting of the letters 'KWR' in a bold, blue, sans-serif font.

February 2024 ©

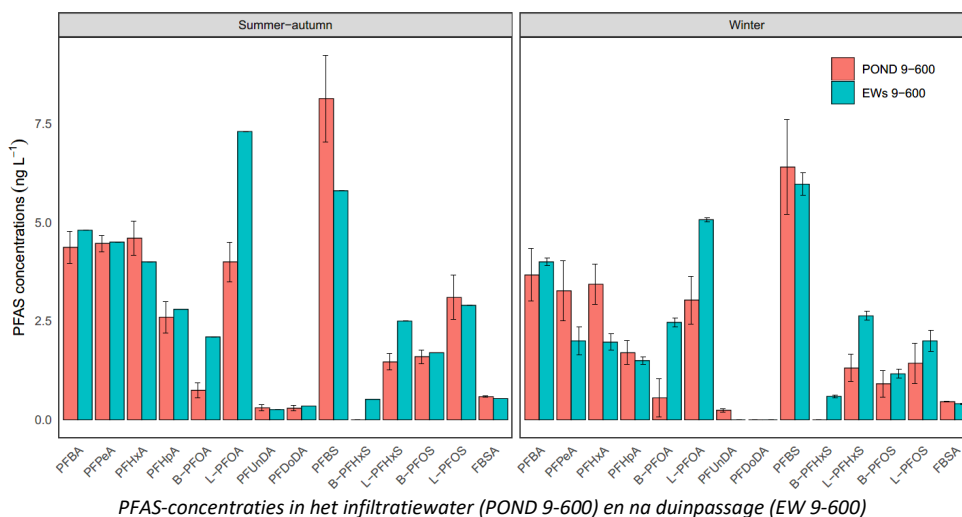
All rights reserved by KWR. No part of this publication may be reproduced, stored in an automatic database, or transmitted in any form or by any means, be it electronic, mechanical, by photocopying, recording, or otherwise, without the prior written permission of KWR.

Managementsamenvatting

Toename PFAS tijdens duininfiltratie mogelijk door nalevering uit de bodem?

Auteurs: Elvio Amato, Bas van der Grift

Bodempassage door de duinen resulteert consequent in hogere PFAS concentraties in het opgepompte water dan in het geïnfiltreerde oppervlaktewater. Deze toename wordt voornamelijk veroorzaakt door specifieke PFAS-verbindingen, met name L-PFHxS en L-PFOA. Er is geen aantoonbaar verschil gevonden tussen een ruwwaterstreng die vrijwel volledig wordt gevoed door infiltratiewater en een streng met toestroom van natuurlijk grondwater. Het bemonsterde natuurlijke grondwater had lagere PFAS-concentraties dan het geïnfiltreerde oppervlaktewater. Beide waarnemingen suggereren dat toestroom van natuurlijk grondwater momenteel geen significante bron van PFAS is. Nalevering uit de bodem is dan de meest reële oorzaak van de toename tijdens bodempassage. Omdat slechts beperkt grondwatermonsters zijn genomen in het infiltratiegebied en het ondiepe grondwater (met mogelijk hogere PFAS-concentraties) niet is gemeten kan een bijdrage van natuurlijk grondwater ook niet worden uitgesloten. De signatuur van PFAS-gehalten in de bovenste bodemlaag kwam overeen met die uit een eerder onderzoek naar sea spray aerosols (SSA). Dit wijst op een bijdrage van atmosferische depositie aan de PFAS-belasting van de duinen. Om de langetermijnrisico's voor het drinkwater beter in beeld te krijgen is nader onderzoek nodig naar deze belasting, naar de uitspoeling naar het bovenste grondwater en naar de toestroom van dit water naar de onttrekkingsputten.



Belang: gedrag en bronnen PFAS bij duininfiltratie ophelderen

Bij infiltratie in de duinen kunnen natuurlijke processen in de bodem organische micro-verontreinigingen verwijderen, maar duininfiltratie is geen effectieve barrière tegen zeer persistente verontreinigingen als per- en polyfluoralkyl stoffen (PFAS). Bovendien is waargenomen dat PFAS-

concentraties kunnen toenemen na duinpassage, mogelijk als gevolg van de toestroom van grondwater met hogere PFAS-concentraties of nalevering vanuit de bodem tijdens duinpassage. Er is behoefte aan meer kennis over de bronnen en processen in de duinen die PFAS-concentraties kunnen beïnvloeden.

Aanpak: multicompartiment metingen

Oppervlaktewater-, bodem- en grondwatermonsters uit een duininfiltratiegebied zijn geanalyseerd om het lot van PFAS tijdens duininfiltratie te onderzoeken en een meer inzicht te krijgen in de PFAS-verontreiniging in het infiltratiegebied.

Resultaten: hogere concentratie PFAS na infiltratie; potentiële invloed van depositie

De som van de PFAS-concentraties in water dat werd onttrokken na duinpassage was consistent 10 tot 50% hoger dan in het oppervlaktewater dat infiltreert. Er was geen verschil tussen een onttrekkingsstreng midden in het infiltratiegebied die van twee kanten gevoed wordt door infiltratiewater en de onttrekkingsstreng aan de oostkant van het infiltratiegebied die vanuit één kant wordt gevoed door infiltratiewater en vanuit de andere kant door toestroom van natuurlijk grondwater. Deze toename werd voornamelijk veroorzaakt door L-PFOA en L-PFHxS, en wordt mogelijk veroorzaakt door nalevering van PFAS die aan bodemdeeltjes was geadsorbeerd. Toenemende verontreiniging door menging met natuurlijk grondwater is in dit onderzoek niet aangetoond: er is geen verschil gevonden in PFAS-toename tussen beide onttrekkingsstrengen en de gemeten concentraties in het natuurlijke grondwater waren lager dan die in geïnfiltreerd en onttrokken water. De metingen van het natuurlijke grondwater zijn echter uitgevoerd in een relatief klein deel van het infiltratiegebied en het meest ondiepe grondwater is niet meegenomen. Op basis van de bemonsterde locaties is het niet mogelijk om een gebiedsdekkend beeld te krijgen van de PFAS-verontreinigen in het natuurlijk grondwater door atmosferische depositie.

Analyse van bodemmonsters uit het gebied tussen de infiltratiepanden en de onttrekkingsstrengen liet zien dat de PFAS-gehalten in de verzadigde zone minstens 1 orde van grootte lager waren dan die gemeten in de onverzadigde zone. Dit kan wijzen op een lagere PFAS-concentratie in het infiltratiewater, dan in de door atmosferische depositie belaste natuurlijke grondwateraanvulling. Lage PFAS-gehalten in verzadigde grond kunnen echter ook verband houden met 1) andere sorptiemechanismen in de onverzadigde zone in vergelijking met de verzadigde zone (sorptie op het grensvlak tussen

lucht en water beïnvloedt PFAS-gehalten in de onverzadigde zone, maar niet in de verzadigde zone), 2) de mogelijkheid dat het infiltratiewater altijd lagere PFAS-concentraties heeft gehad dan het door atmosferische depositie belaste bodemvocht of 3) een lager gehalte aan bodembestanddelen die PFAS kunnen binden in de verzadigde zone (zoals organische koolstof of ijzeroxiden), wat mogelijk een gevolg is van uitloging door langdurige infiltratie van oppervlaktewater. Er werden consistente concentratiepatronen waargenomen tussen de toplaag van de bodem en eerdere PFAS-metingen uitgevoerd in zeespray-aërosolen (SSA) (BTO 2023.047), wat suggereert dat depositie van SSA waarschijnlijk een belangrijke bron van PFAS in het duingebied is. De PFAS-gehalten in de onverzadigde zone namen geleidelijk af met toenemende diepte: dit duidt op een langzame en stofspecifieke uitspoeling van PFAS vanaf het maaiveld naar diepere bodemlagen. Dit is ook een aanwijzing dat atmosferische depositie een belangrijke bron is van de PFAS-verontreiniging in het duingebied. Een bijdrage van deze bron aan de PFAS-concentratie in het ruwwater is in dit onderzoek niet aangetoond, maar kan ook niet worden uitgesloten.

Toepassing: depositie en transportmechanismen in de bodem achterhalen

Het is bekend dat kustduinen onder invloed staan van atmosferische depositie van SSA. Verder onderzoek is nodig om de PFAS-depositieflux te kwantificeren en te achterhalen welke invloed die heeft op de PFAS-concentraties in het natuurlijke grondwater, hoe dat bijdraagt aan de PFAS-concentratie in uit de duinen opgepompt ruwwater en hoe zich dit in de toekomst gaat ontwikkelen. Dit vereist een beter begrip van (ruimtelijke) patronen in atmosferische depositie en transportmechanismen in de bodem, vooral in de onverzadigde zone en ondiep grondwater. Hiervoor is een beter begrip nodig van de verdeling van PFAS tussen de vaste fase en de waterfase en de adsorptie op het grensvlak tussen lucht en water. Een continuering van het uitgevoerde (BTO 2022.056 en BTO 2023.029) en lopende onderzoek naar gedrag van PFAS in bodems is hiervoor noodzakelijk.

Het rapport

Dit onderzoek is beschreven in het rapport *Fate of PFAS in dune infiltration* (KWR 2024.044).

Contents

| | |
|--|-----------|
| Report | 2 |
| <i>Managementsamenvatting</i> | 3 |
| Contents | 5 |
| 1 Introduction | 6 |
| 2 Material and methods | 7 |
| 2.1 Chemicals and reagents | 7 |
| 2.2 Surface water and groundwater sampling | 7 |
| 2.3 Soil and sediment sampling | 8 |
| 2.4 Sample preparation and analysis | 9 |
| 3 Results and discussion | 11 |
| 3.1 PFAS concentrations in soil and sediment cores | 11 |
| 3.2 PFAS occurrence in surface water and groundwater | 13 |
| 3.2.1 General trends | 13 |
| 3.2.2 Pond water | 13 |
| 3.2.3 Groundwater in monitoring wells | 14 |
| 3.2.4 Groundwater in extraction wells | 14 |
| 3.2.5 Natural groundwater | 14 |
| 3.3 Fate of PFAS during dune infiltration | 14 |
| 3.4 Potential PFAS contamination sources | 16 |
| 4 Conclusions | 18 |
| References | 19 |

1 Introduction

There is much concern about per- and polyfluoroalkyl substances (PFAS) in the environment and their potential effects on human health and biota. These compounds typically partition to the aqueous phase and are thus challenging to remove from water (Lenka et al., 2021). In addition, PFAS are very persistent to (biological) degradation in the environment and are commonly not removed by processes such as dune or bank filtration. However, it is unknown whether this applies also to PFAS precursors, which may potentially be converted into more stable PFAS.

Routine monitoring data collected by the drinking water company PWN suggested that PFAS concentrations increase upon filtration through coastal dunes. This was attributed to potential contributions from deposition of sea-spray aerosols (SSA) (Sha et al., 2022), and prompted a preliminary investigation that found PFAS contamination in SSA collected on the Dutch coast (Amato et al., 2023). While evidence suggested links between SSA and PFAS contamination in air, transport mechanism across the different compartments of the dune infiltration area (i.e., air, soil, and groundwater) are not understood yet. Research on transport mechanisms in the unsaturated and saturated zones showed that leaching of PFAS from topsoil to groundwater is retarded by compound specific adsorption on surfaces of soil particles or interfaces between air and water (Van Leeuwen et al., 2022, Van Leeuwen et al., 2023). Recent research has also shown that the dunes may become a source of organic micropollutants after a decrease of concentrations in the influent water due to remobilisation of adsorbed substances from the soil matrix (Grift and Meekel, 2023). Decreasing concentrations in influent water from the river Rhine have been observed also for some common PFAS such as PFOA, PFOS, PFBA, PFBS, PFHxS (Grift and Meekel, 2023; Van Driezum et al., 2024)

Currently, no soil monitoring studies have been specifically performed in dune infiltration systems, and uncertainty remains on the general occurrence of PFAS in the dunes (i.e., stock and storage), their transport, accumulation, and potential release to groundwater. Due to their tendency to partition to water, PFAS are not expected to be strongly retained in soil (except for PFAS with longer carbon chains ($C > 7$)), and thus, these substances are likely to move with the water and seep through the soil reaching groundwater (Dauchy et al., 2019; Richardson et al., 2022).

In this study, we investigated the occurrence of PFAS in soil, sediment, and groundwater in the dune infiltration area of PWN in Wijk aan Zee. The behaviour of PFAS during dune infiltration was assessed by comparing concentrations measured before and after dune infiltration. For the most part, this assessment considered estimated groundwater travel times. Since PFAS in extraction wells from the edge of the infiltration area – where infiltrated water mixes with natural groundwater – were reported to be higher than those measured in the extraction wells from the middle section of the area, PFAS contamination in natural groundwater was investigated as well.

2 Material and methods

2.1 Chemicals and reagents

Samples were analysed for 30 target PFAS and perfluorinated compounds. These included perfluoro-n-butanoic acid (PFBA), perfluoro-n-pentanoic acid (PFPeA), perfluoro-n-hexanoic acid (PFHxA), perfluoro-n-heptanoic acid (PFHpA), perfluoro-n-octanoic acid (PFOA), perfluoro-n-nonanoic acid (PFNA), perfluoro-n-decanoic acid (PFDA), perfluoro-n-undecanoic acid (PFUnDA), perfluoro-n-dodecanoic acid (PFDoDA), perfluoro-n-tridecanoic acid (PFTTrDA), perfluoro-n-tetradecanoic acid (PFTeDA), 4:2 fluorotelomer sulfonic acid (4:2 FTS), 6:2 fluorotelomer sulfonic acid (6:2 FTS), 8:2 fluorotelomer sulfonic acid (8:2 FTS), hexafluoropropylene oxide dimer acid (HFPO-DA), 4,8-dioxa-3H-perfluorononanoic acid (NaDONA), 9-chlorohexadecafluoro-3-oxanonane-1-sulfonic acid (9Cl-PF3ONS), 11-chloroeicosafuoro-3-oxaundecane-1-sulfonic acid (11Cl-PF3OUdS), perfluoro-n-butanefulfonic acid (PFBS), perfluoropentane sulfonic acid (PFPeS), perfluoro-n-hexanesulfonic acid (PFHxS), perfluoro-n-heptanesulfonic acid (PFHpS), perfluoro-n-octanesulfonic acid (PFOS), perfluoro-n-nonane sulfonic acid (PFNS), perfluoro-n-decanesulfonic acid (PFDS), perfluoro-1-butanefulfonamide (FBSA), perfluoro-1-hexanesulfonamide (FHxSA), perfluoro-1-octanesulfonamide (FOSA), N-methylperfluorooctanesulfonamidoacetic acid (N-MeFOSAA), N-ethylperfluorooctanesulfonamidoacetic acid (N-EtFOSAA). In addition, also branched molecules were reported for PFOS, PFHxS and PFOA, although the results for these compounds are semiquantitative. Mass-labelled internal standard (IS) consisting of a mixture of 19 carboxylic and sulphonic PFAS were purchased from Wellington Laboratories (Ontario, Canada). The IS HFPO-DA-¹³C₃ was supplied by Greyhound Chromatography and Allied Chemicals (Birkenhead, United Kingdom). Ammonium hydroxide solution (NH₄OH) was obtained from Sigma Aldrich. Ultrapure water (LiChrosolv®), LC-MS grade was obtained from Merck (Zwijndrecht, The Netherlands).

2.2 Surface water and groundwater sampling

Surface water samples (500 mL) were collected from (i) an infiltration pond located on the furthest east side of the infiltration dune in section 9-600 (POND 9-600), and (ii) from a pond located in the centre of the infiltration area, in section 10-400 (POND 10-400) (Figure 1). Groundwater extracted in section 9-600 is comprised of approximately 2/3 of infiltrated groundwater and 1/3 of groundwater from natural dunes surrounding the infiltration area. Surface water samples from the pond of section 9-600 were collected 3 times over a period of 36 days (details on sampling dates are provided in Annex I). This sampling window was within the time required for groundwater to travel from the pond to the extraction wells of row 9-600, which was estimated to be 45 days. After complete passage of groundwater across the infiltration dune, groundwater samples from extraction well 9-608 (Figure 2) were collected for additional 35 days. This allowed to sample approximately the same water previously collected in the infiltration pond. On day 45, 2 additional monitoring wells (L5111 and W821) located in the natural dunes next to extraction well 9-608, as well as 2 monitoring wells (L5146 and L5133) located between the pond and the extraction wells of sections 9-600 and 10-400 were sampled (Figure 2). The depth of each filter is reported in Annex I. The travel time from the pond to well L5146 and L5133 was estimated to be approximately 9 days. Finally, samples from the combined water of the wells of section 9-600 (EWs 9-600) were also collected (1 in summer-autumn and 3 in winter). In summer-autumn, it was originally planned to collect 3 samples from EW 9-608, however, due to technical issues, 2 samples from EW 9-608 and 1 sample from EWs 9-600 were collected. To account for seasonal variability, the same sampling was performed in late summer-autumn (July - October) and winter (December - March). Samples were collected in polypropylene (PP) bottles and stored frozen until analysis.



Figure 1. Overview of the PWN infiltration area.



Figure 2. Locations of the groundwater and surface water sampling (left = internal dune, right = external dune).

2.3 Soil and sediment sampling

Soil and sediment core samples of 3.2 cm in diameter were collected using a metal core sampler, divided in segments of ~10 to ~50 cm (Figure 3), and stored in HDPE containers. Two soil core samples were collected on each side of the extraction wells of section 9-600 (EWs 9-600), one from the portion of dune between the extraction wells and its

corresponding feeding pond (POND 9-600) (internal dune), and one from the dune on the east side of EWs 9-600 (external dune). One additional sediment core was obtained from POND 9-600. Soil cores were collected at a maximum depth of 4 m, whereas the sediment core was collected from the middle of the pond at a maximum depth of 2 m from the sediment-water interface, respectively. After sampling, samples were stored at 5 ± 3 °C until analysis. For each core, three sub-samples, corresponding to the top, mid-, and bottom layer of the core, were selected for determination of PFAS concentrations.

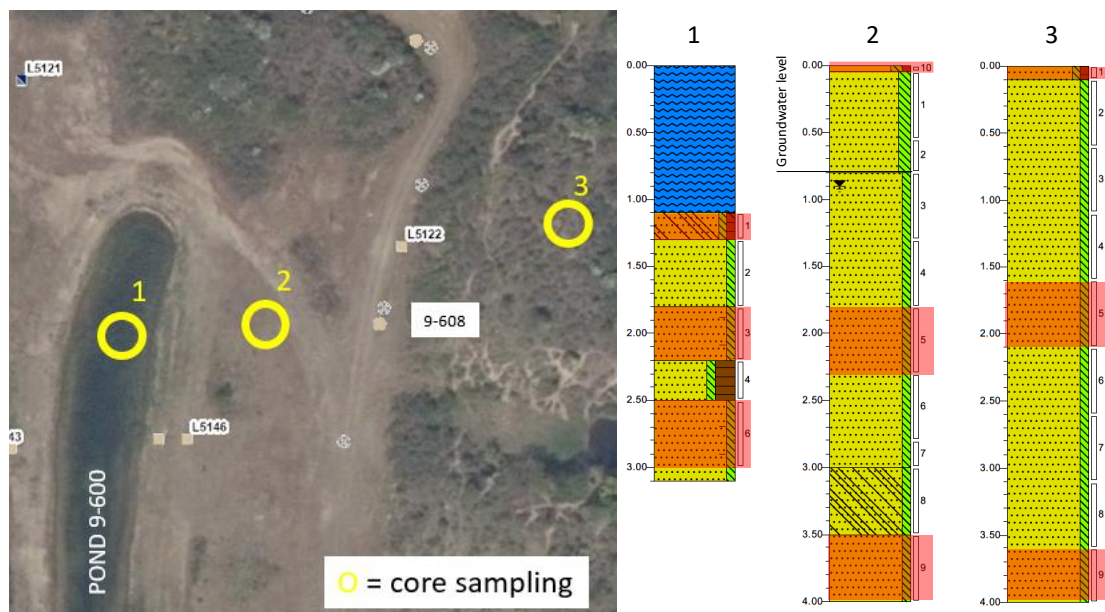


Figure 3. Location of the core sampling (left) and details on cores depth (right). Shaded areas indicate subsamples used for PFAS analysis.

2.4 Sample preparation and analysis

Water samples were allowed to defrost overnight before extraction. Following addition of internal standard (100 μ L mixture of 20 mass-labelled PFAS (20 μ g/L in MeOH) and 100 μ L of HFPO-DA ($^{13}\text{C}_3$, 20 μ g/L in MeOH)), samples were acidified to a pH of 4-5 using HCl. Solid phase extraction (SPE) was carried out using Oasis-WAX SPE cartridges (150 mg, 30 μ m, 6cc, Oasis[®]). The extraction procedure included a precleaning step which was performed using a PP cartridge containing 3 grams of sea sand placed on top of the Oasis-WAX cartridge using an adapter. Before extraction, both cartridges were conditioned using two times 5 mL 0.25% ammonium hydroxide (NH_4OH , 29%) in MeOH followed by two times 5 mL ultrapure water (LC-MS grade). Sand cartridges and adapters were removed and 5 mL of 25 mM ammonium acetate pH 4 was added to the WAX SPE cartridges for cleaning. SPE cartridges were covered with aluminium foil and allowed to dry for 1.5 hours under vacuum. Empty bottles were allowed to dry and rinsed using 10 mL of MeOH. The rinsing solution was transferred to a clean glass tube. The same tube was then used to collect the eluate from the corresponding SPE cartridges. Cartridges were eluted using 5 mL 0.25% ammonium hydroxide (NH_4OH , 29% in MeOH). Eluates (i.e., 15 mL in total) were reduced to a volume of 500 μ L under a gentle stream of nitrogen (Barkey, 67°C). After evaporation, samples were made up to a final volume of 1 mL (MeOH:ultrapure (UP) water 1:1 v/v) spiked with an injection standard (IS) PFAS mixture (i.e., $^{13}\text{C}_3\text{PFBA}$, $^{13}\text{C}_2\text{PFOA}$ and $^{13}\text{C}_4\text{PFOS}$ (4 μ g/L in MeOH)), resulting in a concentration factor of 500x. Samples were then filtered (0.45 μ m, regenerated cellulose, Whatman[®]) and stored in the freezer (-20 °C) until analysis. Procedural blanks were prepared using the bottles filled with ultrapure water and extracted using the procedure described above.

Analyses were performed using a Tribrid Orbitrap Fusion mass spectrometer (ThermoFisher Scientific, Bremen, Germany) equipped with a heated electrospray ionization source interfaced to a Vanquish HPLC system

(ThermoFisher Scientific). The chromatographic analysis was performed using an XBridge BEH C18 XP column (100 mm × 2.1 mm I.D., particle size 2.5 µm, Waters, Etten-Leur, The Netherlands) in combination with a 2.0 mm × 2.1 mm I.D. Phenomenex SecurityGuard Ultra column (Phenomenex, Torrance, USA), maintained at 25°C. Eluent composition was A: 2 mM NH₄Ac in ultrapure-water and B: 2 mM NH₄Ac in methanol:acetonitrile 80:20% (v/v). The LC gradient started with 30% B for 1 min. Then increased to 60% B in 2 min and stayed constant for 4 min. Next, increased to 90% B in 9 min and then increased to 100% B in 1 min and stayed constant for 3 min. Mass spectrometric detection was performed in negative ionization mode. The Vaporizer and capillary temperature was set to 300 °C and 200 °C, respectively. Sheath, auxiliary and sweep gas were set to arbitrary units of 30, 5 and 5 for both RP and MM. The source voltage was set to – 2.5 kV in negative mode. The RF lens was set to 50%. Full scan high resolution mass spectra were recorded from m/z 150–1000, with a resolution of 120'000 FWHM. Quadrupole isolation was used for acquisition with a 5 ppm mass window. The AGC target was set to 200'000 and maximum injection time was set to 100 ms. MS/MS spectra were recorded using a mass table list. Optimal HCD collision energy was selected for each individual PFAS. With every batch run, mass calibration was performed using a Pierce FlexMix calibration solution to obtain a mass error of < 2 ppm. The recovery of the method ranges between 95% and 105% with relative standard deviation (RSD = σ/μ) below 6% for all analytes.

Soil and sediment samples were analysed at Vrij Universiteit Amsterdam. Prior to the analysis the samples were lyophilised and grinded manually. Carbon 13 isotopically labelled internal standard (50 µl, 10 ng/ml) was added to 2.5 gram sample. The samples were extracted twice using a 10 mL mixture of acetonitrile and methanol (1:1, v/v) containing 0.1% ammonium hydroxide. The two extracts were combined and evaporated to dryness, and reconstituted in 1mL methanol. The extracts were cleaned by dispersive SPE with 100 mg graphitized carbon. The supernatant was evaporated to dryness after the cleaning and reconstituted in 50 µl mixture of water and methanol (1:1, v/v). The extracts were injected on an analytical column (Xbridge C18 100x2.1mm, 2.5µm, Waters) by a gradient of 20 mM ammonium acetate and methanol, starting at 25% methanol, and ramping it up to 99% in 10 minutes. The target compounds were detected with a mass selective detector (MS/MS, 6500+, Sciex) using electrospray ionization operated in the negative ion mode. The RSD of this method ranged between 1 and 15%.

3 Results and discussion

3.1 PFAS concentrations in soil and sediment cores

PFAS were found in both soil and sediment core samples (Figure 4). Vertical gradients were observed in all cores, and the general trend indicated higher PFAS concentrations in the top layer compared to the middle and bottom layers (Figure 4). In the sediment, this was consistent with typically higher levels of organic carbon (OC) found at the sediment-water interface, which acts as a binding phase for PFAS (Nguyen et al., 2020). The most abundant PFAS in this layer were the long-chain carboxylic acids PFUnDA, PFNA and PFDoDA, and PFOS (Figure 5), consistently with their higher soil-water partition coefficient (K_d) (Nguyen et al., 2020). In the middle and bottom layer, PFUnDA, PFNA and PFOS were still the most abundant compounds, however, the overall PFAS concentrations (i.e., Σ PFAS concentrations) decreased. In the soil top layer, PFOS was consistently the most abundant compound, followed by PFOA, PFNA, PFDA and PFBA (Figure 5). For perfluoroalkyl carboxylic acids (PFCA), the general trend indicated decreasing concentrations from C4 to C6, followed by an increase from C7 to C8. After C8, concentrations progressively decreased again. Among the PFSA investigated in this study, only PFBS, PFHxS, PFHpS and PFOS were found in these samples. In the mid-layer of the external dune, PFCA concentrations appeared to decrease with increasing number of carbons, i.e., from C4 (PFBA) to C10 (PFDA), except for PFOA which occurred at much higher concentrations (Figure 5). The PFOA concentration measured in this sample was the highest found in the whole core. The same PFSA found in the top layer were also measured in the middle layer, except for PFHpS. A considerable decrease in PFOS levels (from 2.6 to 0.02 $\mu\text{g}/\text{kg}$) was observed in this layer, whereas a large increase in PFBS concentrations was detected in the mid-layer (from 0.03 to 0.8 $\mu\text{g}/\text{kg}$). In the bottom layer of the external dune, detected PFCA ranged from C4 to C9, with PFOA exhibiting the highest concentration (0.32 $\mu\text{g kg}^{-1}$) by a factor of approximately 10. PFOS showed a substantial increase compared to the mid-layer (from 0.02 to 0.2 $\mu\text{g kg}^{-1}$), whereas PFHxS and PFHpS concentrations did not seem to largely vary throughout the whole core. While the two soil samples showed very similar PFAS concentrations in the top layer (except for PFOS), considerable differences were observed in the mid- and bottom layers.

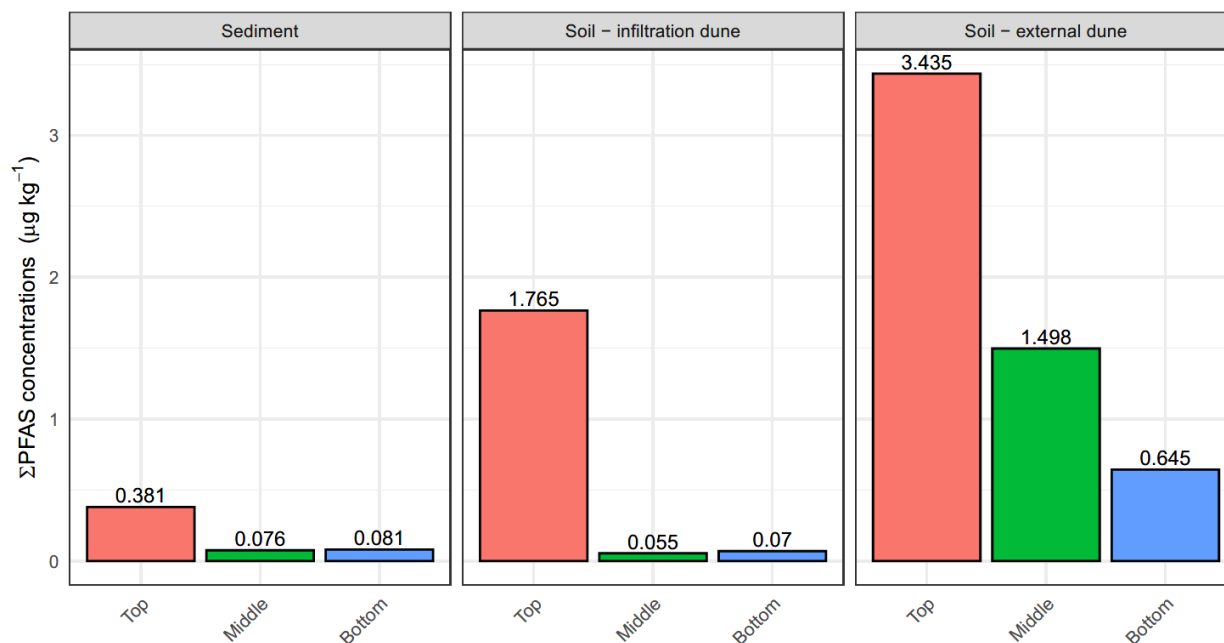


Figure 4. Sum of PFAS concentrations measured in the top, mid- and bottom sections of core samples.

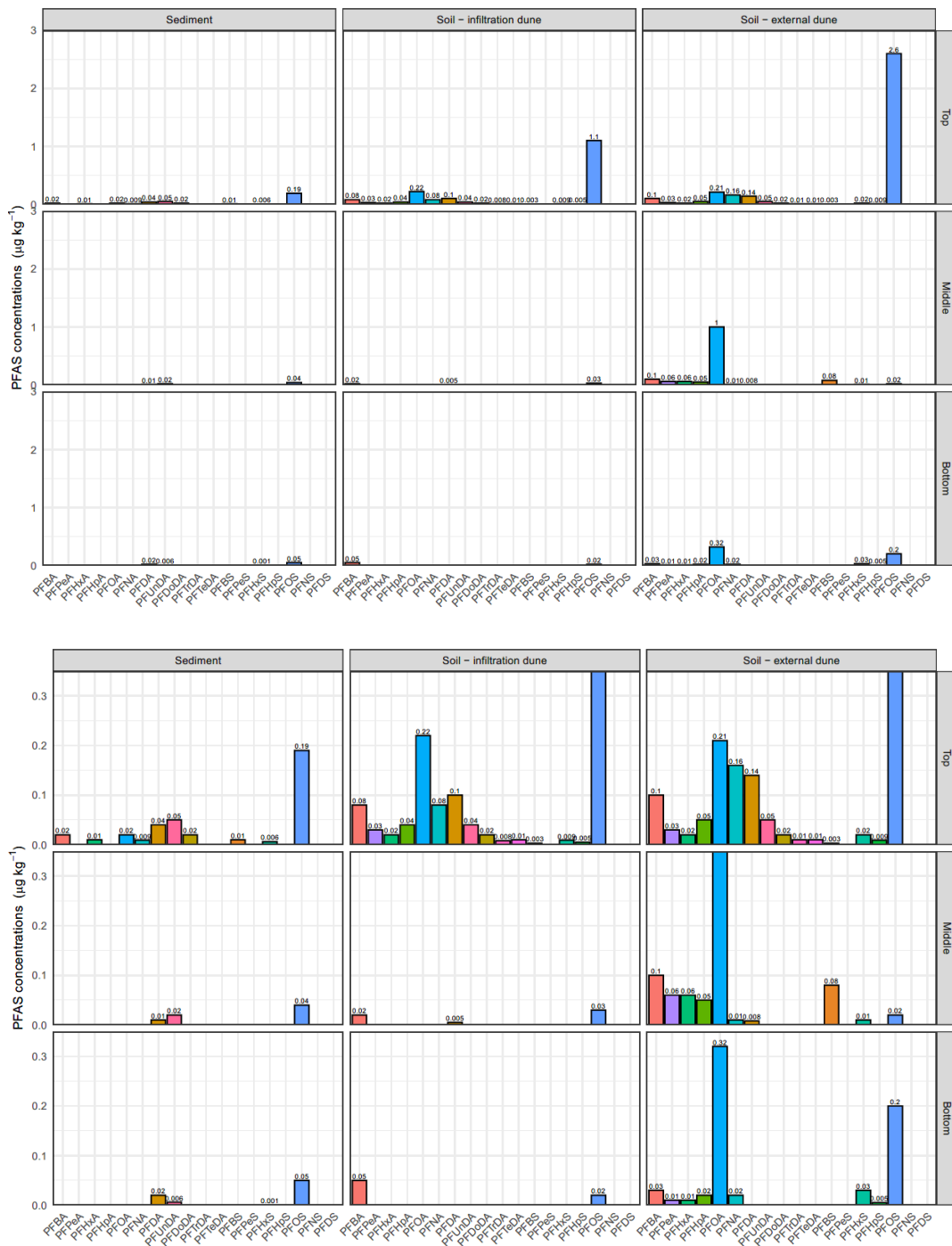


Figure 5. PFAS concentrations measured in the top, mid- and bottom layers of core samples. The top and bottom panel report the same data with different scales. All soil samples were unsaturated except for the middle and bottom layers of the infiltration dune.

In the infiltration dune (Sample 2, Figure 3), these layers were characterized by substantially lower concentrations compared to the external dune (Sample 3, Figure 3, 4 and 5). Since the mid- and bottom layers of the infiltration dune were in the saturated zone (Figure 3), PFAS soil levels in these layers are expected to be regulated by partition equilibrium between soil and water (Annex II). In contrast, this was not observed in the core collected in the external dune, which was characterised by unsaturated soil.

3.2 PFAS occurrence in surface water and groundwater

3.2.1 General trends

Approximately half of the PFAS investigated were consistently found in both surface water and groundwater, including perfluoroalkyl carboxylic acids (PFCA) (PFBA (96%), PFPeS (75%), PFHxA (82%), PFHpA (82%), B-PFOA (79%), and L-PFOA (89%)), perfluoroalkyl sulfonic acids (PFSA) (PFBS (89%), L-PFHxS (86%), B-PFOS (79%), and L-PFOS (79%)), and one perfluorosulfonamide (PFSM) precursor (FBSA (68%)) (percentages indicate the frequency of detection). Additional PFAS included PFUnDA (46%), B-PFHxS (29%), PFDoDA (29%), 6:2 FTS (7%) and 8:2 FTS (7%). All the remaining PFAS were not detected. The most abundant compounds were PFBS, PFBA, L-PFOA, PFHxA, PFPeA and L-PFOS, which were found at median concentrations of 5.8, 3.9, 3.6, 2.2, 2.1 and 1.9 ng/L, respectively. 6:2 FTS occurred only in two samples, EW 10-423 and EW 9-608, at 4.2 and 250 ng/L, respectively (Annex I). The concentration measured in EW 9-608 was > 20 times higher than the second highest concentration measured in this study (PFOA, 15 ng/L). This extremely high concentration, combined with very low detection frequency, appears to indicate potential contamination during field operations or sample handling.

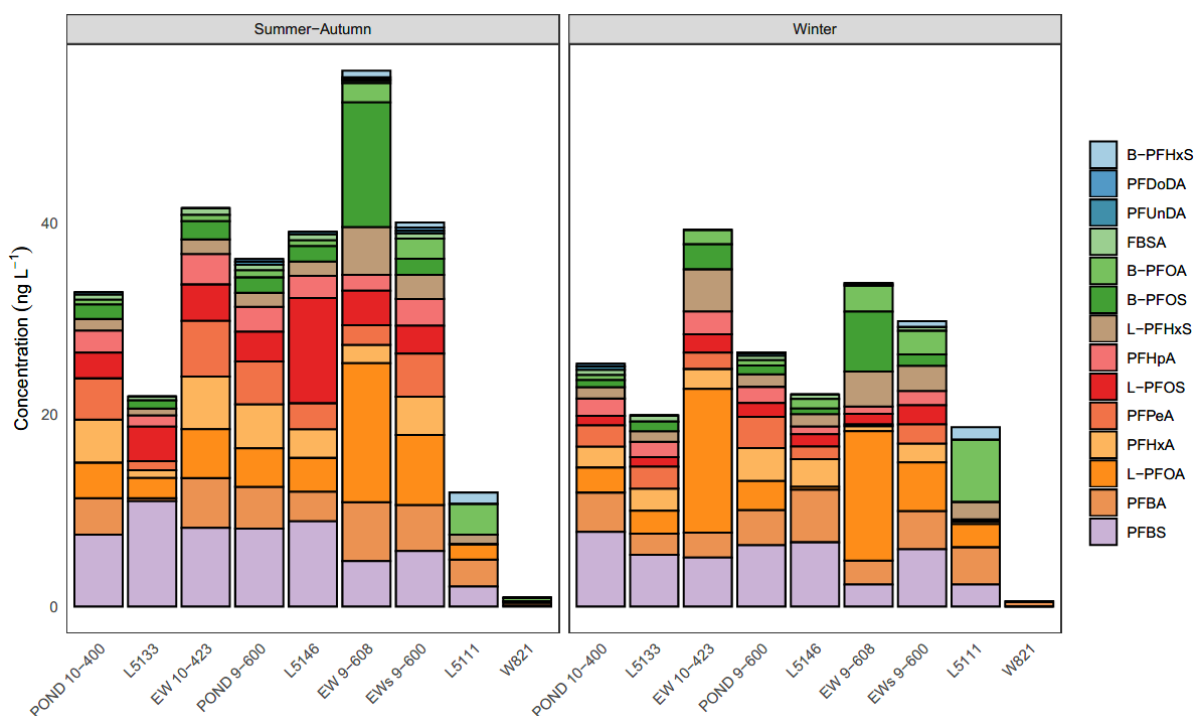


Figure 6. PFAS concentrations measured in surface water (POND 10-400 and POND 9-600) and groundwater (section 10-400: L5133, EW 10-423; section 9-600: L5146, EW 9-608, EWs 9-600; natural groundwater: L5111, W821 (average of 3 depths, see Annex I) samples collected in summer-autumn and winter. Data are means of 3 measurements for POND 9600 (summer-autumn and winter) and EWs 9-608 (winter), 2 measurements for EW 9-608 (summer-autumn and winter), and single measurements for the remaining parameters. To improve data visualization, 6:2 FTS results are omitted from this chart.

3.2.2 Pond water

The sum of PFAS concentrations (Σ PFAS) in samples collected from the infiltration ponds was similar between POND 10-400 and POND 9-600 in winter (25.5 and 26.5 ± 5.7 ng/L, respectively) as well as summer-autumn (32.8 and 36.3 ± 3.3 ng/L, respectively) (Figure 6). For both ponds, the Σ PFAS was higher in summer-autumn compared to winter (Figure 6), and PFBS, PFBA, L-PFOA, PFHxA, and PFPeA were the most dominant compounds. In summer-autumn, the Σ PFAS concentrations in POND 9-600 (36.3 ± 3.3 , RSD = 9%) appeared to be more stable than in winter (26.5 ± 5.7 , RSD = 21%).

3.2.3 Groundwater in monitoring wells

Concentrations in monitoring wells L5133 and L5146 – located between the infiltration ponds and the extraction wells of section 10-400 and 9-600, respectively – were typically lower than those measured in the infiltration ponds and extraction wells, except for L5146 in summer-autumn. This was due in large part to the exceptionally high concentration of L-PFOS (11 ng/L), which was approximately 3 times higher than the concentration measured in the same well in winter (3.6 ng/L), and 10 times higher than the concentrations measured in the monitoring well located near to POND 10-400 (1.0 - 1.3 ng/L). In general, L-PFOS levels in this sample exceeded those measured in the whole sampling campaign for this compound (≤ 4.1 ng/L, $n = 27$) by a factor > 2.7 .

3.2.4 Groundwater in extraction wells

The highest PFAS levels were consistently found in the groundwater collected in extraction wells (EW 10-423 and 9-608), where Σ PFAS concentrations ranged from 41.6 to 57.5 ng/L. In summer-autumn, concentrations in EW 9-608 (57.5 ng/L) were higher than those measured in EW 10-423 (41.6 ng/L), whereas in winter, the opposite trend was observed (35.2 and 39.6 ng/L for EW 9-608 and 10-423, respectively). However, in summer-autumn, samples were collected 12 days apart (Annex I), and thus, did not account for groundwater residence time (which is assumed to be approximately the same for section 9-600 and 10-400). B-PFOS levels in EW 9-608 (13.0 ng/L) were almost 10 times higher than those measured in POND 9-600 (1.6 ng/L) and L5146 (1.6 ng/L), and in winter, 6- to 10-fold (6.3 ng/L) higher than those measured in POND 9-600 (0.9 ng/L) and L5146 (0.6 ng/L). This was not observed in the combined water from all the wells of section 9-600 (i.e., EWs 9-600), suggesting the presence a localised source of B-PFOS in this area. In EWs 9-600, the Σ PFAS concentrations was lower than EW 9-608, but higher than POND 9-600 and L5146 (Figure 6), for both summer-autumn and winter samples. The difference in PFAS concentrations between EWs 9-600 and EW 9-608 suggests that heterogeneous contamination may be expected within the same group of extraction wells.

3.2.5 Natural groundwater

Natural groundwater was characterized by considerably lower contamination levels compared to other samples from the infiltration area (Figure 6). Well L5111 contained higher levels of PFAS (11.9 - 18.7 ng/L) compared to W821 (0.23 - 2.31 ng/L) (Annex I). This may be linked to the different depth of the filters (i.e., L5111 much shallower than W821, Annex I), and thus, to the different age of the groundwater (Annex I). Assuming that PFAS enter the dunes via atmospheric deposition, shallower groundwater is expected to be more contaminated than deeper groundwater. Concentrations in these wells appeared to be lower in summer-autumn (0.23 - 11.9 ng/L) than winter (0.53 - 18.7 ng/L). For L5111, detected PFAS included PFBA, PFBS, B-PFHxS, L-PFHxS, PFHxA, PFHpA, B-PFOA, and L-PFOA. In W821, only PFBA (0.3 - 0.5 ng/L) and PFUnDA (0.23 ng/L) were found in the shallowest screen (W821-F1) and mid-screen (W821-F2), and only PFBA (0.6 ng/L), PFBS (0.3 ng/L), B-PFOA (0.98 ng/L) and L-PFOA (0.48 ng/L) in the deepest screen (W821-F3), respectively (Annex I). A distinct characteristic of natural groundwater was the greater relative abundance of branched PFOA and PFHxS over the corresponding linear molecules. This may be linked to the higher mobility of branched molecules compared to linear ones, however, further investigations are needed to support this hypothesis. In L5111, B-PFOA (3.2 - 6.5 ng/L) and B-PFHxS (1.2 - 1.3 ng/L) occurred at greater or similar concentrations compared to L-PFOA (1.6 - 2.4 ng/L) and L-PFHxS (1.0 - 1.8 ng/L) (Annex I). In W821, higher B-PFOA concentrations were also found in the deepest screen (i.e., 1.0 and 0.5 ng/L for B-PFOA and L-PFOA, respectively).

3.3 Fate of PFAS during dune infiltration

Direct comparisons between water samples can be done when groundwater travel times between pond and extraction wells are taken into account. This applied to (i) POND 9-600, EW 9-608, and EWs 9-600 (45 days), (ii) POND 10-400 and EW 10-423 (only in summer-autumn, 45 days), (iii) POND 9-600 and L5146 (9 days), and (iv) POND 10-423 and L5133 (only winter, 9 days) (Annex I). In section 9-600, a considerable increase in B-PFOA, L-PFOA, and L-PFHxS concentrations was observed upon passage across the dunes (Figure 7).

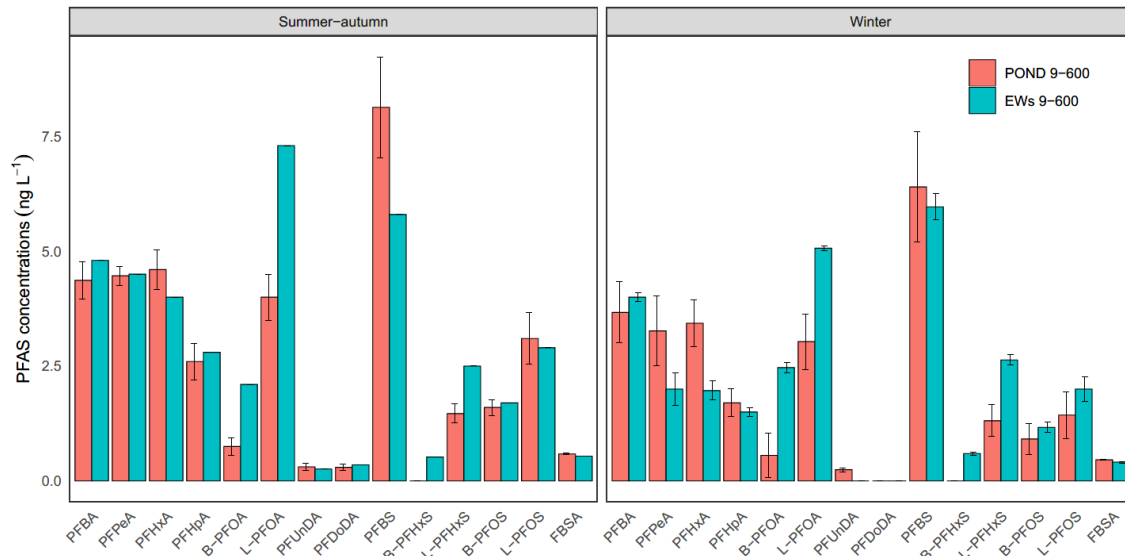


Figure 7. Comparison between PFAS concentrations before and after infiltration in the dunes of section 9-600 (means \pm SD, $n = 3$; for EWs 9-600 in summer-autumn, $n = 1$). To improve data visualization, 6:2 FTS results are omitted from this chart.



Figure 8. PFAS concentrations measured in pond water and groundwater in different sections of the dune infiltration area. To improve data visualization, 6:2 FTS results are omitted from this chart.

In this comparison, the retardation of PFAS by sorption to the soil particles was not taken into account. It is known that retardation factors of PFAS have a substantial variation and increase with the CF_2 chain length. In case of the dune infiltration system, with relatively short travel times of the water between infiltration of the water and abstraction, combined with a history of PFAS loading of several decades, it can be assumed that the soil matrix has been saturated with PFAS for a long time. Additional adsorption of PFAS from recently infiltrated water is therefore of minor importance, which makes the comparison of water samples along the flowline between infiltration and abstraction possible. An increase in concentration between infiltration and abstraction can occur due to desorption from the soil particles. This process has recently been identified as the cause of an increase in concentrations of metabolites of some banned pesticides during dune infiltration (Van der Grift & Meekel, 2023), following decreasing concentration in the influent water; thus, decreasing concentrations in the influent may also be responsible for the observed increase in PFAS.

A moderate increase was also detected for B-PFOS, L-PFOS, and B-PFHxS. In contrast, decreasing concentrations were measured for PFPeA and PFHxA in winter. While dilution with less contaminated natural groundwater may be expected in EWs 9-600 (Figure 6), lower PFPeA, PFHxA, and PFHpA concentrations were also observed in L5146 (Figure 8). This was even more evident when considering EW 9-608 (Figure 8), where decreasing PFPeA, PFHxA and PFHpA were consistently observed in both summer-autumn and winter. Since these compounds are not expected to strongly bind to soil (Nguyen et al., 2020), it is unclear what factors may contribute to decreasing groundwater concentrations. For the remaining PFAS, no substantial changes were observed upon dune passage (Figure 7).

In section 10-400, increasing concentrations were measured from POND 10-400 to EW 10-423 for almost all detected compounds in summer-autumn (Figure 8). In winter, increasing concentrations were mainly observed for L-PFOA, L-PFHxS, and B-PFOS, although care should be taken when interpreting these results because winter monitoring did not take into account groundwater travel times between POND 10-400 and EW 10-423 (Figure 8). In contrast, travel times were considered between POND 10-400 and L5133 in winter (i.e., 9 days), and results indicated decreasing concentrations between these two sampling points (Figure 6 and 8). In summer-autumn, most PFAS occurred at much lower concentrations in L5133 compared to POND 10-400. While this specific comparison did not account for groundwater travel time, results were overall consistent with measurements in winter (Figure 6).

3.4 Potential PFAS contamination sources

The comparison between PFCA concentrations measured in the soil top layer and in sea-spray aerosol (SSA) indicated a similar increasing trend from C6 to C8, followed by decreasing concentrations from C8 to C14 (Figure 9). Also PFSA concentrations were consistent between soil top layer and SSA (Figure 9). These patterns may suggest that SSA deposition could be an important source of contamination in the dunes. In addition, PFBA was measured in soil at relatively high concentrations, but was not detected in SSA. This may indicate the presence of additional sources or processes contributing to PFBA contamination in the dune area. In contrast, 6:2 FTS and HFPO-DA were detected in aerosols samples, but not in soil.

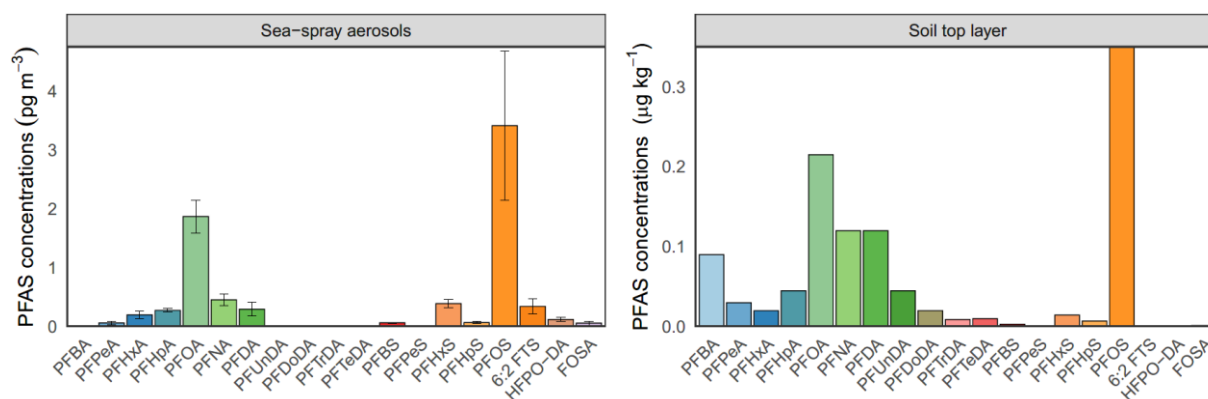


Figure 9. PFAS concentrations measured in sea-spray aerosols (mean \pm SD, $n = 8$) (Amato et al., 2023) and in the soil top layer (mean, $n = 2$).

Previous studies have shown that biotransformation of precursors such as 6:2 FTS may take place in soil, and contribute to the formation of more stable PFAS, such as PFBA (Shaw et al., 2019; Zhang et al., 2021; Zhao et al., 2021). Furthermore, non-target screening analysis tentatively annotated several potential polyfluoroalkyl acid (PFAA) precursors in aerosol samples collected in the Wijk aa Zee infiltration area (Amato and Béen, 2023). These results highlight the need to investigate the potential impact of precursors to PFAS contamination levels in coastal dunes.

Due to the relatively low PFAS concentrations measured in natural groundwater, it seems unlikely that natural groundwater may contribute to increasing PFAS concentrations in infiltrated water. However, only a small section of the dune infiltration area was investigated in this study. While PFOA, PFOS and PFHxS increased in concentration upon passage through the dune, other compounds such as PFPeA, PFHxA and PFHpA appeared to decrease in the localised area near EW 9-608, although it is unclear what mechanisms may contribute to this effect.

4 Conclusions

This study showed that PFAS concentrations in groundwater extracted upon dune passage was consistently higher than that measured in surface water entering the dune infiltration area. The Σ PFAS varied between 25.5–36.3 ng/L in the infiltration ponds and 35.2–57.5 ng/L in the extracted groundwater. L-PFHxS and L-PFOA were the main contributors of this increase. There was no clear difference in both the level of Σ PFAS concentration and the increase in Σ PFAS concentration between the extraction well section in the middle of the infiltration area (section 10-400), that is mainly fed by infiltration water, and the extraction section on the east border of the infiltration area (section 9-600), that is also fed by natural groundwater. This indicates that flow of natural groundwater towards the extraction wells does not result in an increase in PFAS concentration. Remobilisation of adsorbed PFAS during dune infiltration is then the most likely cause of this increase.

Differences were observed between one extraction well from section 9-600 (EW 9-608) and the combined water from all extraction wells of section 9-600 (EWs 9-600), suggesting heterogeneous PFAS concentrations within the same section of the infiltration area. EW 9-608 was characterised by elevated levels of B-PFOS, which was not particularly abundant in other wells. This heterogeneous presence of PFAS was also observed in groundwater samples from monitoring wells between the infiltration ponds and the extraction sections, which typically showed lower Σ PFAS concentrations.

Natural groundwater sampled from monitoring wells in the dune area on the eastern side of the infiltration area showed relative low PFAS concentrations. The Σ PFAS in the shallow groundwater at 8 m depth ranged from 11.9 to 18.7 ng/L and in the deeper groundwater between 15 and 40 m depth from 0.23 to 2.31 ng/L. Since concentrations in these wells were lower than those measured in infiltrated water, natural groundwater is not expected to contribute to increased PFAS levels in abstracted water. However, it should be noted that the most shallow groundwater that likely contains the highest concentration of PFAS was not sampled in this monitoring campaign. The same applies for the natural groundwater in the external dune area at the sea side of the infiltration area that is likely most affected by deposition of SSA enriched in PFAS.

The PFAS content in the unsaturated soil samples from the external dune area decreased with depth. This suggests that concentrations in the groundwater may increase over time due to leaching processes. PFAS patterns in the soil top layer were consistent with those of SSA reported in a previous study, suggesting potential contributions from deposition of SSA. PFAS precursors were also previously reported in air samples, and the potential impact of (bio)transformation of PFAS precursors to more stable PFAS in infiltration dunes should be investigated. The precursor 6:2 FTS was detected at very high concentrations in EW 9-608 (250 ng/L) and EW 10-423 (4.2 ng/L), but was not detected in other samples. This was attributed to potential contamination during field sampling, however, close monitoring of this compound is recommended.

Finally, considerably lower PFAS contents were measured in soil samples from the saturated zone between the infiltration pond and the abstraction well, compared to samples collected in the unsaturated zone. This could be attributed to: (i) higher PFAS concentrations in precipitation water that infiltrates in the unsaturated zone, (ii) lower content of PFAS binding phases – such as organic carbon or iron-oxides – in the saturated zone, potentially due to leaching processes due to long term infiltration of surface water, or (iii) PFAS sorption at the air-water interface which impacts the PFAS concentration in the unsaturated zone, but not in the saturated zone.

References

- Amato, E.D., Béen, F., 2023. Non-targeted screening of PFAS in sea-spray aerosols. KWR Water Research Institute.
- Amato, E.D., Béen, F., Vughs, D., 2023. PFAS in sea-spray aerosols, BTO 2023.47. KWR Water Research Institute.
- Dauchy, X., Boiteux, V., Colin, A., Hémar, J., Bach, C., Rosin, C., Munoz, J.-F., 2019. Deep seepage of per- and polyfluoroalkyl substances through the soil of a firefighter training site and subsequent groundwater contamination. *Chemosphere* 214, 729–737. <https://doi.org/10.1016/j.chemosphere.2018.10.003>
- Driezum, I., van, Van der Grift, B., Cirkel, G. en Pronk, T. (2024) Grondwaterkwaliteit bij grootschalige infiltratie oppervlaktewater. KWR BTO 2024.045.
- Grift, B. van der, Meekel, N., 2023. Verkenning verhoogde concentraties organische microverontreinigingen na duinpassage, BTO 2023.054. KWR Water Research Institute.
- Leeuwen, J. van, Stofberg, S., van der Grift, B., en Hartog, N. (2023) Verkenning uitspoeling van diffuse PFAS verontreiniging voor onverzadigde bodems in Nederland KWR BTO 2023.029
- Leeuwen, J., van, van der Grift, B. en Been, F. (2022) Kennisdocument PFAS gedrag bodems. KWR rapport BTO 2022.056.
- Lenka, S.P., Kah, M., Padhye, L.P., 2021. A review of the occurrence, transformation, and removal of poly- and perfluoroalkyl substances (PFAS) in wastewater treatment plants. *Water Research* 199, 117187. <https://doi.org/10.1016/j.watres.2021.117187>
- Nguyen, T.M.H., Bräunig, J., Thompson, K., Thompson, J., Kabiri, S., Navarro, D.A., Kookana, R.S., Grimison, C., Barnes, C.M., Higgins, C.P., McLaughlin, M.J., Mueller, J.F., 2020. Influences of Chemical Properties, Soil Properties, and Solution pH on Soil–Water Partitioning Coefficients of Per- and Polyfluoroalkyl Substances (PFASs). *Environ. Sci. Technol.* 54, 15883–15892. <https://doi.org/10.1021/acs.est.0c05705>
- Richardson, M.J., Kabiri, S., Grimison, C., Bowles, K., Corish, S., Chapman, M., McLaughlin, M.J., 2022. Per- and Poly-Fluoroalkyl Substances in Runoff and Leaching from AFFF-Contaminated Soils: a Rainfall Simulation Study. *Environ. Sci. Technol.* 56, 16857–16865. <https://doi.org/10.1021/acs.est.2c05377>
- Sha, B., Johansson, J.H., Tunved, P., Bohlin-Nizzetto, P., Cousins, I.T., Salter, M.E., 2022. Sea Spray Aerosol (SSA) as a Source of Perfluoroalkyl Acids (PFAAs) to the Atmosphere: Field Evidence from Long-Term Air Monitoring. *Environ. Sci. Technol.* 56, 228–238. <https://doi.org/10.1021/acs.est.1c04277>
- Shaw, D.M.J., Munoz, G., Bottos, E.M., Duy, S.V., Sauvé, S., Liu, J., Van Hamme, J.D., 2019. Degradation and defluorination of 6:2 fluorotelomer sulfonamidoalkyl betaine and 6:2 fluorotelomer sulfonate by *Gordonia* sp. strain NB4-1Y under sulfur-limiting conditions. *Science of The Total Environment* 647, 690–698. <https://doi.org/10.1016/j.scitotenv.2018.08.012>
- Zhang, W., Pang, S., Lin, Z., Mishra, S., Bhatt, P., Chen, S., 2021. Biotransformation of perfluoroalkyl acid precursors from various environmental systems: advances and perspectives. *Environmental Pollution* 272, 115908. <https://doi.org/10.1016/j.envpol.2020.115908>
- Zhao, S., Liu, T., Zhu, L., Yang, L., Zong, Y., Zhao, H., Hu, L., Zhan, J., 2021. Formation of perfluorocarboxylic acids (PFCAs) during the exposure of earthworms to 6:2 fluorotelomer sulfonic acid (6:2 FTSA). *Science of The Total Environment* 760, 143356. <https://doi.org/10.1016/j.scitotenv.2020.143356>

Annex I

PFAS concentrations measured in surface water and groundwater samples (ng/L).

| Sampling date | Sample | Filter depth (m) | 6:2 FTS | 8:2 FTS | FBSA | PFBA | PFBS | PFDoDA | PFHpA | PFHpS | PFHxA | B-PFHxS | L-PFHxS | B-PFOA | L-PFOA | B-PFOS | L-PFOS | PFPeA | PFUnDA |
|---------------|--------------|------------------|---------|---------|--------|------|--------|--------|--------|--------|--------|---------|---------|--------|--------|--------|--------|--------|--------|
| Summer-Autumn | | | | | | | | | | | | | | | | | | | |
| 25-07-2022 | POND 10-400 | - | < 1.0 | < 0.5 | 0.6 | 3.8 | 7.5 | < 0.50 | 2.3 | < 0.50 | 4.5 | < 0.50 | 1.2 | 0.5** | 3.7 | 1.5** | 2.7 | 4.3 | 0.2* |
| 08-09-2022 | L5133 | 6.25 | < 1.0 | < 0.5 | 0.4 | 0.3 | 11.0 | < 0.50 | 1.2 | < 0.50 | 0.8 | < 0.50 | 0.7 | < 0.50 | 2.1 | 0.8** | 3.6 | 0.9 | < 0.50 |
| 08-09-2022 | EW 10-PUT423 | 6.4 | < 1.0 | < 0.5 | 0.7 | 5.2 | 8.2 | < 0.50 | 3.2 | < 0.50 | 5.5 | < 0.50 | 1.5 | 0.7** | 5.1 | 1.9** | 3.8 | 5.8 | < 0.50 |
| 25-07-2022 | POND 9-600 | - | < 1.0 | < 0.5 | 0.58 | 3.9 | 7.5 | 0.25* | 2.2 | < 0.50 | 4.3 | < 0.50 | 1.3 | 0.63** | 3.5 | 1.4** | 2.5 | 4.3 | 0.22* |
| 16-08-2022 | POND 9-600 | - | < 1.0 | < 0.5 | 0.61 | 4.6 | 7.5 | 0.37* | 2.6 | < 0.50 | 4.4 | < 0.50 | 1.7 | 0.97** | 4.5 | 1.7** | 3.6 | 4.4 | 0.39* |
| 30-08-2022 | POND 9-600 | - | < 1.0 | < 0.5 | 0.57 | 4.6 | 9.4 | 0.27* | 3.0 | < 0.50 | 5.1 | < 0.50 | 1.4 | 0.65** | 4 | 1.7** | 3.2 | 4.7 | 0.31* |
| 08-09-2022 | L5146 | 4.48 | < 1.0 | < 0.5 | 0.62 | 3.1 | 8.9 | < 0.50 | 2.3 | < 0.50 | 3.0 | < 0.50 | 1.5 | 0.62** | 3.5 | 1.6** | 11 | 2.7 | 0.26* |
| 08-09-2022 | EWs 9-600 | - | < 1.0 | 0.21* | 0.54 | 4.8 | 5.8 | 0.35* | 2.8 | < 0.50 | 4.0 | 0.52** | 2.5 | 2.1** | 7.3 | 1.7** | 2.9 | 4.5 | 0.26* |
| 20-09-2022 | EW 9-608 | 7.05 | < 1.0 | < 0.5 | 0.22* | 6.3 | 4.6 | < 0.50 | 1.7 | 0.53* | 2.0 | 0.71** | 5.2 | 1.8** | 15 | 14** | 3.1 | 2.3 | < 0.50 |
| 13-10-2022 | EW 9-608 | 7.05 | < 1.0 | < 0.5 | 0.28* | 6 | 4.9 | 0.41* | 1.6 | 0.33* | 1.8 | 0.64** | 4.8 | 2.2** | 14 | 12** | 4.1 | 1.8 | 0.35* |
| 08-09-2022 | L5111 | 8.42 | < 1.0 | < 0.5 | < 0.50 | 2.8 | 2.1 | < 0.50 | < 0.50 | < 0.50 | < 0.50 | 1.2** | 1.0 | 3.2** | 1.6 | < 0.50 | < 0.50 | < 0.50 | < 0.50 |
| 09-09-2022 | W821-F1 | 15.5 | < 1.0 | < 0.5 | < 0.50 | 0.34 | < 0.50 | < 0.50 | < 0.50 | < 0.50 | < 0.50 | < 0.50 | < 0.50 | < 0.50 | < 0.50 | < 0.50 | < 0.50 | < 0.50 | < 0.50 |
| 09-09-2022 | W821-F2 | 22.47 | < 1.0 | < 0.5 | < 0.50 | 0 | < 0.50 | < 0.50 | < 0.50 | < 0.50 | < 0.50 | < 0.50 | < 0.50 | < 0.50 | < 0.50 | < 0.50 | < 0.50 | < 0.50 | 0.23* |
| 09-09-2022 | W821-F3 | 37.93 | < 1.0 | < 0.5 | < 0.50 | 0.57 | 0.28* | < 0.50 | < 0.50 | < 0.50 | < 0.50 | < 0.50 | < 0.50 | 0.98** | 0.48 | < 0.50 | < 0.50 | < 0.50 | < 0.50 |
| Winter | | | | | | | | | | | | | | | | | | | |
| 17-01-2023 | POND 10-400 | - | < 1.0 | 0.21* | 0.55 | 4.1 | 7.8 | 0.28* | 1.8 | < 0.50 | 2.2 | < 0.50 | 1.2 | 0.54** | 2.6 | 0.72** | 1 | 2.2 | 0.34* |
| 26-01-2023 | L5133 | 6.25 | < 1.0 | < 0.5 | 0.64 | 2.2 | 5.4 | < 0.50 | 1.6 | < 0.50 | 2.3 | < 0.50 | 1.1 | < 0.50 | 2.4 | 1** | 1 | 2.3 | < 0.50 |
| 26-01-2023 | EW 10-PUT423 | 6.4 | 4.2 | < 0.5 | < 0.50 | 2.6 | 5.1 | < 0.50 | 2.4 | 0.25* | 2.1 | < 0.50 | 4.4 | 1.5** | 15 | 2.6** | 1.9 | 1.7 | < 0.50 |
| 12-12-2022 | POND 9-600 | - | < 1.0 | < 0.5 | 0.47* | 4.1 | 7.6 | 0.27* | 2.0 | < 0.50 | 3.9 | < 0.50 | 1.6 | 0.84** | 3.6 | 1.3** | 2.0 | 4.1 | 0.29* |
| 03-01-2023 | POND 9-600 | - | < 1.0 | < 0.5 | 0.46* | 4 | 6.4 | < 0.50 | 1.7 | < 0.50 | 3.5 | < 0.50 | 1.4 | 0.83** | 3.1 | 0.75** | 1.3 | 3.1 | 0.2* |
| 17-01-2023 | POND 9-600 | - | < 1.0 | < 0.5 | 0.45* | 2.9 | 5.2 | < 0.50 | 1.4 | < 0.50 | 2.9 | < 0.50 | 0.93 | < 0.50 | 2.4 | 0.69** | 1 | 2.6 | 0.24* |
| 26-01-2023 | L5146 | 4.48 | < 1.0 | < 0.5 | 0.47* | 5.5 | 6.7 | < 0.50 | 0.8 | < 0.50 | 2.9 | < 0.50 | 1.3 | 1.0** | 0.29* | 0.57** | 1.3 | 1.3 | < 0.50 |
| 26-01-2023 | EWs 9-600 | - | < 1.0 | < 0.5 | 0.39* | 3.9 | 6.3 | < 0.50 | 1.6 | < 0.50 | 2.2 | 0.62** | 2.7 | 2.4** | 5.1 | 1.3** | 2.3 | 2.4 | < 0.50 |
| 17-02-2023 | EWs 9-600 | - | < 1.0 | < 0.5 | 0.42* | 4 | 5.8 | < 0.50 | 1.5 | < 0.50 | 1.9 | 0.56** | 2.5 | 2.4** | 5.0 | 1.1** | 1.8 | 1.9 | < 0.50 |

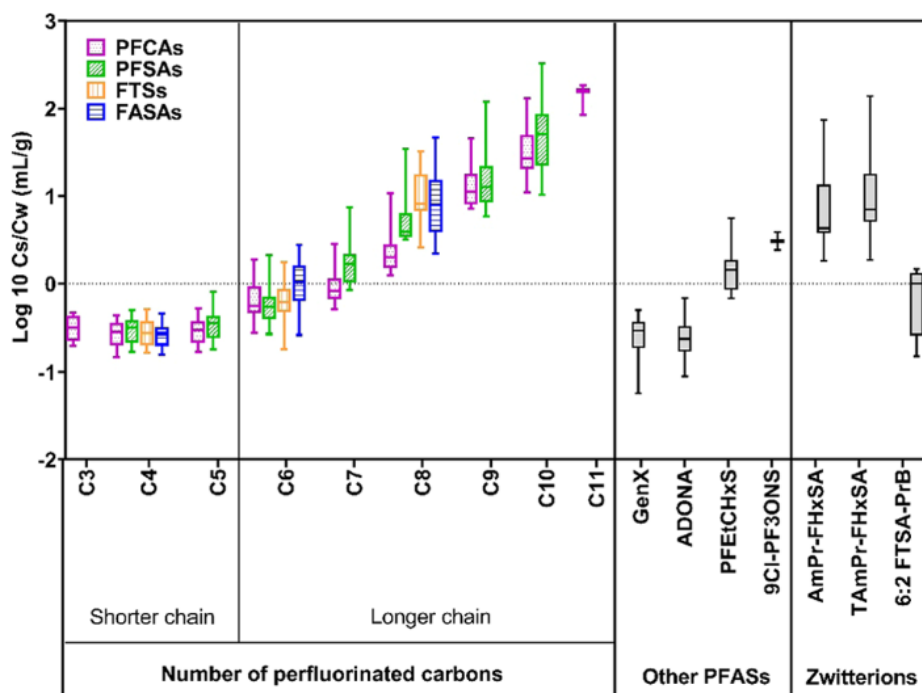
| | | | | | | | | | | | | | | | | | | | |
|------------|-----------|------|-------|-------|--------|------|--------|--------|--------|--------|--------|--------|--------|--------|--------|--------|--------|--------|--------|
| 03-03-2023 | EWs 9-600 | - | < 1.0 | < 0.5 | 0.42* | 4.1 | 5.8 | < 0.50 | 1.4 | < 0.50 | 1.8 | 0.61** | 2.7 | 2.6** | 5.1 | 1.1** | 1.9 | 1.7 | < 0.50 |
| 26-01-2023 | EW 9-608 | 7.05 | 250 | < 0.5 | < 0.50 | 2 | 2.3 | 0.29* | 0.69 | 0.26* | 0.52 | < 0.50 | 4.1 | 2.8** | 14 | 6.5** | 1.4 | < 0.50 | 0.31* |
| 03-03-2023 | EW 9-608 | 7.05 | < 1.0 | < 0.5 | < 0.50 | 3 | 2.3 | < 0.50 | 0.84 | 0.21* | 0.53 | < 0.50 | 3.2 | 2.6** | 13 | 6.0** | 0.8 | 0.37* | 0 |
| 17-01-2023 | L5111 | 8.42 | < 1.0 | < 0.5 | < 0.50 | 3.9 | 2.3 | < 0.50 | 0.23* | < 0.50 | 0.28* | 1.3** | 1.8 | 6.5** | 2.4 | < 0.50 | < 0.50 | < 0.50 | 0 |
| 17-01-2023 | W821-F1 | 15.5 | < 1.0 | < 0.5 | < 0.50 | 0.53 | < 0.50 | < 0.50 | < 0.50 | < 0.50 | < 0.50 | < 0.50 | < 0.50 | < 0.50 | < 0.50 | < 0.50 | < 0.50 | < 0.50 | 0 |

Compounds always found below the LOQ (reported in brackets in ng/L): 11Cl-PF3OUdS (0.50), 4:2 FTS (0.50), 9Cl-PF3ONS (0.50), DONA (0.50), FHxSA (0.50), FOSA (0.50), HFPO-DA (0.50), N-EtFOSAA (0.50), N-MeFOSAA (0.50), PFDA (4.0), PFDS (0.50), PFNA (2.0), PFNS (0.50), PFPeS (0.50), PFTeDA (3.0), PFTrDA (3.0).

*semiquantitative results (< LOQ).

** semiquantitative results (sum of branched isomers, non-validated results)

Annex II



Box plots of logarithm (base 10) transformed K_d values for 29 PFASs in up to 10 soils as a function of perfluorinated C-chain length for PFCAs, PFASs, FTSS, and FASAs (colored) together with other PFASs and zwitterions (gray). The boxes and whiskers represent median and minimum to maximum values, respectively; $n = 3$ for C11 PFCA, $n = 2$ for 9Cl-PF3ONS, $n = 9$ for zwitterions, and $n = 10$ for remaining compounds; n is the number of soils (Nguyen et al., 2020).